

ELECTRON BEAM PATTERN ROTATION AS A METHOD OF TUNABLE BUNCH TRAIN GENERATION

A. Halavanau^{1,2}, P. Piot^{1,2}

¹ Department of Physics and Northern Illinois Center for Accelerator & Detector Development, Northern Illinois University DeKalb, IL 60115, USA

² Fermi National Accelerator Laboratory, Batavia IL 60510, USA

Abstract

Transversely modulated electron beams can be formed in photo injectors via microlens array (MLA) UV laser shaping technique. Microlenses can be arranged in polygonal lattices, with resulting transverse electron beam modulation mimicking the lenses pattern. Conventionally, square MLAs are used for UV laser beam shaping, and generated electron beam patterns form square beamlet arrays. The MLA setup can be placed on a rotational mount, thereby rotating electron beam distribution. In combination with transverse-to-longitudinal emittance exchange (EEX) beam line, it allows to vary beamlets horizontal projection and tune electron bunch train. In this paper, we extend the technique to the case of different MLA lattice arrangements and explore the benefits of its rotational symmetries.

INTRODUCTION

Emittance exchange beamline provides the mapping between $(\mathbf{X}, \mathbf{X}') \leftrightarrow (\mathbf{Z}, \delta')$ phase spaces while $(\mathbf{Y}, \mathbf{Y}')$ phase space being unaffected by the exchange. This technique is commonly used for controllable longitudinal bunch train generation in many applications [1–10].

A typical EEX setup consists of two dipoles (first “dogleg”) that followed by a time deflecting cavity (TDC1), which is in turn followed by two more dipoles (second “dogleg”). Under thin-elements approximation the transfer matrix of the EEX beamline can be written as:

$$\mathbf{R}_{x \rightarrow z} = \begin{pmatrix} 0 & 0 & (L+L_d)\kappa & \eta + (L+L_d)\kappa\zeta \\ 0 & 0 & \kappa & \zeta\kappa \\ \zeta\kappa & \eta + (L+L_d)\kappa\zeta & 0 & 0 \\ \kappa & (L+L_d)\kappa & 0 & 0 \end{pmatrix}.$$

Here L is the path length through the dogleg and L_d is the path length between the dipole and the TDC. The transverse-to-longitudinal transfer then can be explicitly written as:

$$z_f = -\frac{\xi}{\eta}x_i - \frac{L\xi - \eta^2}{\eta}x'_i, \quad (1)$$

where (η, ξ) are horizontal (vertical) dispersions, (x_i, x'_i) is the particle’s initial position in transverse phase space, z_f is the corresponding longitudinal coordinate. Thus, a modulation in x -projection of the particle’s transverse distribution will result in longitudinal density modulation. Note, that in Eq. (1) longitudinal coordinate z takes very simple form and doesn’t depend on geometrical parameters of the EEX setup when $x' = 0$. Hereafter, we will use the dispersion values

of the Argonne Wakefield Accelerator (AWA) EEX beamline $\eta = 0.9$ m and $\xi = 0.33$ m [11]. Additionally, we will assume the condition the waist $x' = 0$ in our simulations.

Recently a new method of forming multi-beam arrays of electron beamlets using microlens arrays (MLAs) have been reported [12]. With a combination of optical elements, such a setup can produce arbitrary electron beam transverse modulation. Additionally, the setup allows for the beam pattern rotation via MLA rotation, providing additional degree of freedom in bunch train generation. In this paper, we explore the effect of different beamlet arrangements prior to EEX beamline on resulting longitudinal density modulation.

We investigated the patterns of electron beamlets depicted in Fig. 1. A regular square lattice with a spacing of $d = 2.5$ mm shown in Fig. 1a was experimentally produced and sent through the AWA EEX [13]. The multi-beam arrangement presented in Fig. 1b can be formed via commercially available hexagonal MLAs. The patterns displayed in Figs. 1c and 1d could be generated with a laser mask at the photocathode or tungsten mask in the beamline.

NUMERICAL SIMULATIONS

We now demonstrate our numerical method for the case of square multi-beam lattice and the identical procedure can be applied to other lattices. Consider a square lattice of spacing d , then the radius vector of each point of the lattice can be parametrized as $r = d\sqrt{n^2 + m^2}$, where n, m are some integers. The x -coordinate of each lattice point is then transformed as $x_{m,n} = (dn \cos \theta - dm \sin \theta)$ under clockwise rotation transformation, where θ is the angle of rotation. For a given (m, n) pair of numbers we generate the resulting transverse density function as

$$F(x, \theta) = F_0 \sum_{m,n} e^{-\frac{(x-x_{m,n})^2}{2\sigma^2}}, \quad (2)$$

where F_0 is the normalization constant and $\sigma = 0.1$ mm which corresponds to the experimentally reported size of electron beamlets in [12]. For the case of a square 5×5 lattice the transverse density function is shown in Fig. 2a. In case of beam waist at the entrance of the EEX setup, the transverse-to-longitudinal transformed density profile is then $F(z, \theta) = -(\xi/\eta)F(x, \theta)$ and the spectral content is defined by:

$$F(\omega, \theta) = \int F(z/c) e^{-i\omega z/c} d(z/c). \quad (3)$$

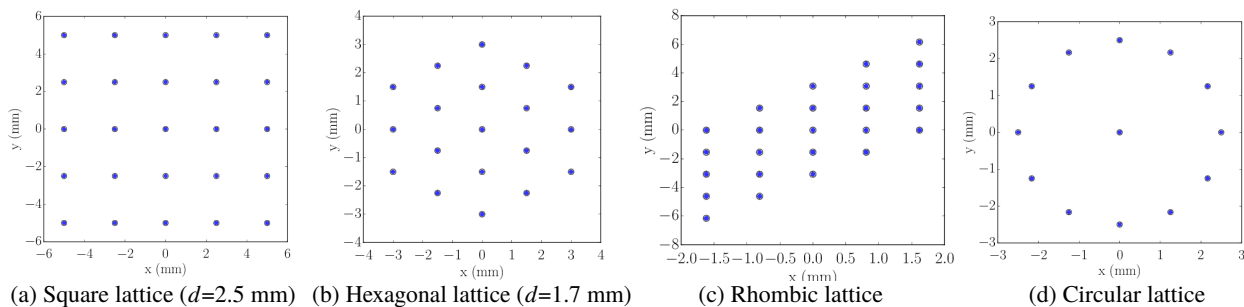


Figure 1: Electron multi-beam distributions arranged in square, hexagonal, rhombic and circular (12 beamlets at 2.5-mm radius) lattices.

A code to compute Eq. (3) for the lattices provided in Fig. 1 was implemented in PYTHON. The resulting functions $F(z/c, \theta)$ and $F(\omega, \theta)$ are displayed in Fig. 2. Following a convention, we will denote $F(\omega, \theta)$ as a longitudinal bunching factor. Note, that this is a very simplified numerical model that doesn't include the effects of beam charge, emittance and longitudinal energy spread. These studies go beyond the scope of this paper and will be reported elsewhere. It should be noted, however, that the lattice spacing and the gaussian beamlets size was selected based on the previously obtained experimental data.

RESULTS

As it can be inferred from Fig. 2 the multi-beam rotation technique can generate tunable multi-beams. For the case of a square arrangement, given the symmetries of the initial laser distribution, a rotation within $0-\pi/4$ is sufficient to explore the entire possible frequency range. However, since the intensity of the laser beamlets in practice may be not consistent within multi-beam array, it is plausible to perform full $0-\pi/2$ rotation. An upright square multi-beam orientation results in 5 nominal peaks displayed in Fig. 2a. In this case, the bunch train separation generated by the EEX setup is equal to $\tau = 4.5$ ps. As it can be inferred from Fig. 2b, the corresponding bunch train time separation at $\theta = \pi/4$ is shrunk by factor of $\sqrt{2}$. Interestingly, the peculiar modulation is generated around $\theta = 26$ deg. The resulting bunching factor $F(\omega, \theta)$ is presented in Fig. 2c and it has a distinct “fishing net”-like structure. It can be concluded that in the case of a square multi-beam lattice one can generate multiple frequencies of the density modulation via pattern rotation.

In the case of hexagonal lattice the density modulation is depicted in Fig. 2d. One should note this type of a lattice generates triangular current profile envelope. Similar current profile may be obtained at $\theta = \pi/4$ with a square lattice. When rotated (see Fig. 2e) it forms a complicated structure due to compactness of the hexagonal lattice. Well defined density modulation can be seen around $\theta = \pi/3$. The resulting bunching factor, presented in Fig. 2f forms a peculiar “tortoise”-like structure. One can note the well-defined harmonics in the spectrum around $\omega = 1$ THz, however,

higher-frequency harmonics have significantly smaller amplitudes. In conclusion, hexagonal lattice can serve for a single-frequency bunch train generation.

The rhombic lattice depicted in Fig. 1c due to its initial xy correlation forms an interesting time profile with increasing modulation wavelength with increasing angle θ ; see Fig. 2h. This method results in “color gradients” in the longitudinal bunching factor; see Fig. 2i. Due to the large number of parameters of the lattice, it may be optimized for a specific gradient. Additionally, many features may arise in the spectrum due to the complexity of the lattice.

A circular lattice presented in Fig. 1d results in the density modulation profile Fig. 2j which contains multiple modulation wavelengths. When rotated (see Fig. 2k) it forms a feature-rich structure that results, for instance in two- and three color radiation frequencies. The shape of the bunching factor is similar to the case of a hexagonal lattice. However, due to regularity of the features, this type of the multi-beam arrangement can be potentially interesting for the improvement of the FEL performance similarly to Ref. [14].

SUMMARY

We demonstrated a simple technique for bunch train generation in the EEX setup using a rotation of the MLA-produced transverse multi-beam array. In particular, we investigated four different multi-beam formations (square, hexagonal, rhombic and circular) under the feasible beam conditions. We found that square and hexagonal lattices can produce different frequencies in the longitudinal density modulation dependent on the angle of rotation. We also considered a rhombic lattice for the “color-gradient” longitudinal spectral content. In case of a circular lattice it was found that two- and three-color modulation can be obtained. We note that the presented method is not limited by the selected lattices.

ACKNOWLEDGEMENTS

This work was supported by the US Department of Energy under contract No. DE-SC0011831 with Northern Illinois University. The work by the AWA group is funded through the U.S. Department of Energy, Office of Science, under contract No. DE-AC02-06CH11357. The work of A.H. and partially P.P. is supported by the US Department of Energy

Content from this work may be used under the terms of the CC BY 3.0 licence (© 2018). Any distribution of this work must maintain attribution to the author(s), title of the work, publisher, and DOI.

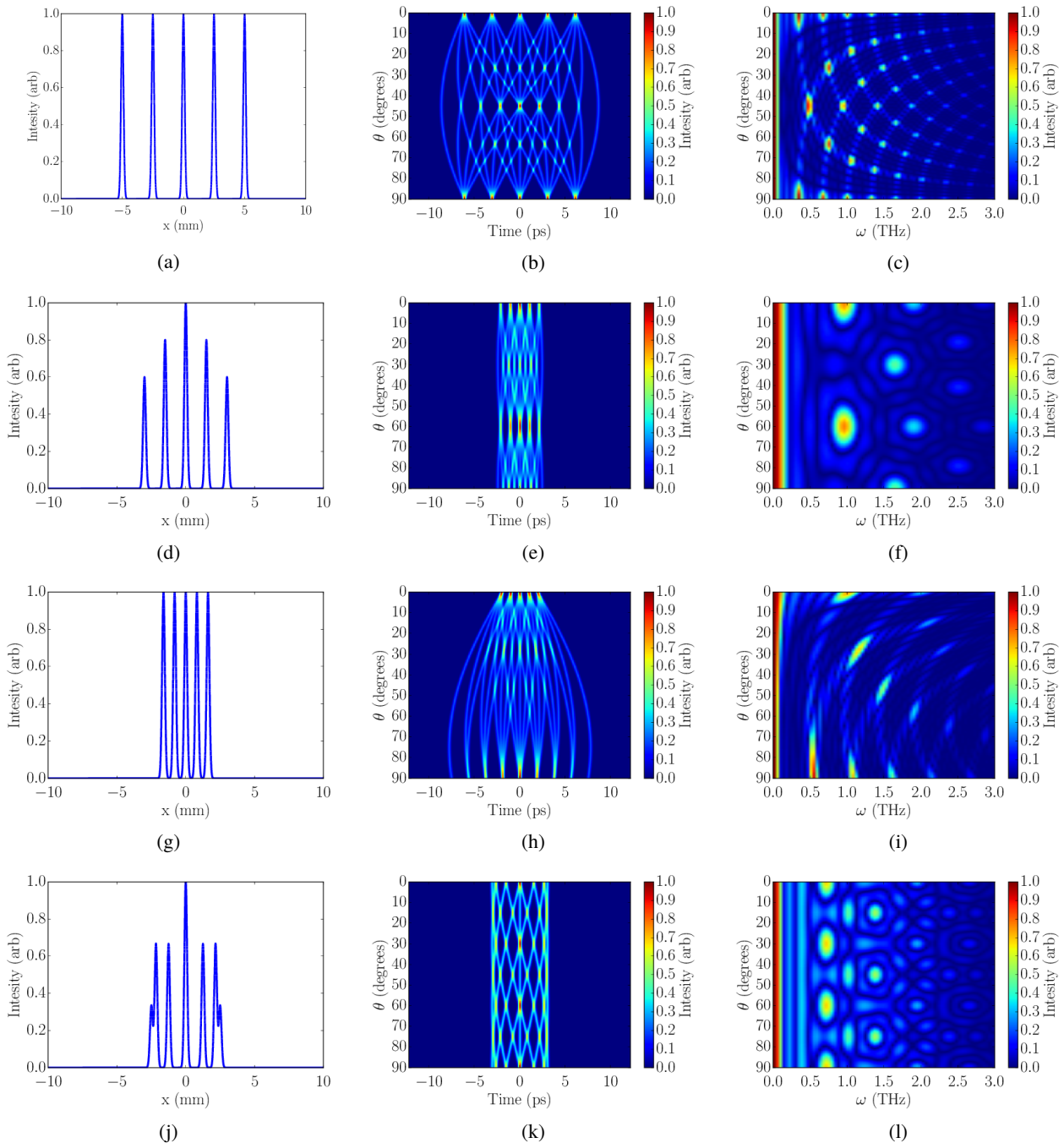


Figure 2: The x -projection of transverse density distribution for $\theta = 0$ degrees (left column), the x -projection as a function of rotation angle θ (middle column), resulting electron bunch spectral content after the EEX as a function of rotation angle θ (right column) for the case of square, hexagonal, rhombic and circular lattices (top to bottom).

under contract No. DE-AC02-07CH11359 with Fermi Research Alliance, LLC. A.H. is grateful to Yuri Pisarchyk (Google), V. Khodygo (Aberystwyth University, UK) and V. Stepanov (B. I. Stepanov Institute of Physics) for the useful mathematical discussions.

REFERENCES

- [1] V. N. Litvinenko and Yaroslav S. Derbenev, “Coherent electron cooling”, *Phys. Rev. Lett.*, **102**, p. 114801, 2009.
- [2] L.-H. Yu *et al.*, “High-gain harmonic-generation free-electron laser”, *Science*, **289** (5481), pp. 932–934, 2000.
- [3] C. Jing *et al.*, “Observation of enhanced transformer ratio in collinear wakefield acceleration”, *Phys. Rev. Lett.*, **98**, p. 144801, 2007.
- [4] P. Piot *et al.*, “Generation and characterization of electron bunches with ramped current profiles in a dual-frequency superconducting linear accelerator”, *Phys. Rev. Lett.*, **108**, p. 034801, 2012.
- [5] J. G. Power, Wei Gai, and Paul Schoessow, “Wakefield excitation in multimode structures by a train of electron bunches”, *Phys. Rev. E*, **60**, pp. 6061–6067, 1999.
- [6] M. Tzoufras *et al.*, “Beam loading in the nonlinear regime of plasma-based acceleration”, *Phys. Rev. Lett.*, **101**, p. 145002, 2008.
- [7] S. Antipov *et al.*, “Experimental demonstration of energy-chirp compensation by a tunable dielectric-based structure”, *Phys. Rev. Lett.*, **112**, p. 114801, 2014.
- [8] P. Piot, Y.-E. Sun, J. G. Power, and M. Rihaoui, “Generation of relativistic electron bunches with arbitrary current distribution via transverse-to-longitudinal phase space exchange”, *Phys. Rev. ST Accel. Beams*, **14**, p. 022801, 2011.
- [9] Yin-e Sun, “Angular-momentum-dominated electron beams and flat-beam generation”, Ph.D. thesis, University of Chicago, 2005.
- [10] T. J. Maxwell, “Measurement of sub-picosecond electron bunches via electro-optic sampling of coherent transition radiation”, Ph.D. thesis, Northern Illinois University, 2012.
- [11] G. Ha *et al.*, “Precision control of the electron longitudinal bunch shape using an emittance-exchange beam line”, *Phys. Rev. Lett.*, **118**, p. 104801, 2017.
- [12] A. Halavanau *et al.*, “Spatial control of photoemitted electron beams using a microlens-array transverse-shaping technique”, *Phys. Rev. Accel. Beams*, **20**, p. 103404, Oct 2017.
- [13] A. Halavanau *et al.*, “Transverse-to-longitudinal photocathode distribution imaging”, in *Proc. of IPAC2018*, Vancouver, Canada, paper THPAK060, 2018, these proceedings.
- [14] P. Emma, Z. Huang, K.-J. Kim, and P. Piot, “Transverse-to-longitudinal emittance exchange to improve performance of high-gain free-electron lasers”, *Phys. Rev. ST Accel. Beams*, **9**, p. 100702, 2006.